THE ASTROPHYSICAL JOURNAL, 430:L117–L120, 1994 August 1

UIT: ULTRAVIOLET OBSERVATIONS OF THE SMALL MAGELLANIC CLOUD

ROBERT H. CORNETT,[1] J. K. HILL,[1] RALPH C. BOHLIN,[2] ROBERT W. O'CONNELL,[3]
MORTON S. ROBERTS,[4] ANDREW M. SMITH,[5] AND THEODORE P. STRECHER[5]
Received 1994 April 4; accepted 1994 May 10

ABSTRACT

UIT far-ultraviolet (FUV) and near-ultraviolet (NUV) images are presented for a 40′ field at the southwest end of the SMC centered near the Hα emission object Henize 19. Photometry is obtained for 1309 stars common to the FUV ($\lambda_{\rm eff} = 1620$ Å) and NUV ($\lambda_{\rm eff} = 2490$ Å) images. We use UIT photometry and imagery to derive a UV color-magnitude diagram for hot field stars; confirm the consistency of low-metal-abundance stellar evolutionary models with the observations; study dust distribution in the field, finding an increase in $E(B-V)$ from the northeast to the southwest; confirm for a large number of stars an extinction curve, like that derived by Hutchings for the SMC, which rises steeply from NUV to FUV; and derive a mass function for SMC field stars and its lack of dependence on assumed extinction curve characteristics. The mass function has a slope within the accepted range ($\Gamma = -1.7 \pm 0.5$) over a wide range of assumed extinction parameters, including variations of the size ($\pm \sim 1.5$ mag $\times$ $E(B-V)$ in the FUV) seen in the Galaxy.

Subject headings: extinction — galaxies: individual (Magellanic Clouds) — galaxies: luminosity function, mass function — ultraviolet: general

1. INTRODUCTION

UV observations above Earth's atmosphere are vital for understanding the SMC. It has long been known, from optical-band data, that the SMC is an excellent laboratory for studying stellar characteristics because it has a well-defined distance and a distinct and extreme composition, compared to the Galaxy. Many effects of composition differences appear best, or only, in the UV. Line blanketing strongly affects UV colors; similarly, the steep SMC extinction curve, widely thought to be due to abundances in SMC dust, is "extreme" only in the UV.

Here we directly confront SMC stellar models and UV extinction curves, until now based on UV spectrographic observation of a few dozen stars, with photometry of 1309 stars by UIT. Broad-band UV observations in critical wavelength ranges, though not as deep or precise as optical ones, delineate effects of composition on stellar colors, define the SMC extinction curve, and clearly show extinction variations across the SMC despite small $E(B-V)$. In addition, UV photometry of hot stars is much more sensitive to stellar mass than optical photometry, and permits investigation of the field mass distribution.

2. OBSERVATIONS AND DATA REDUCTION

UIT observed a 40′ diameter field in the southwest SMC during the Astro-1 mission on 1990 December 4 (Stecher et al. 1992). Eight exposures were made with the UIT B1, B5, and A1 filters, with a total exposure time of less than 200 s (due to Spacelab operational problems). The longest exposures made with the B5 (117 s) and A1 (23 s) filters are used in this study. These images are hereafter called the FUV [$\lambda_{\rm eff} = 1620$ Å; magnitudes $m(162)$] and NUV [$\lambda_{\rm eff} = 2490$ Å; magnitudes $m(249)$] images, and have resolutions (FWHM) of 3″.1 and 2″.9, respectively. Figure 1 (Plate 8) shows the FUV image with outlined locations and sizes of associations as listed in Table 1 of Hodge (1985).

UIT film images are reduced to linearized arrays as described in Stecher et al. (1992). An IDL/UIT implementation of DAOPHOT (Stetson 1987; Hill et al. 1993) is used to locate stars and perform aperture and PSF-fitted photometry. Both aperture and PSF-fitted photometry use a 3″.4 (3 pixel) radius, which sets the limit for resolution of blended stars and the minimum size for nonstellar sources. PSF-fitted photometry, using parameters derived for images individually, is used for subsequent analysis. Astrometric solutions are derived for UIT images using *HST* guide stars as standards (Lasker et al. 1989).

Zero-point corrections for the UIT magnitudes combine aperture corrections and absolute calibration. They are determined by integrating well-exposed and calibrated (Bohlin et al. 1990) *IUE* spectra of seven to nine isolated field stars over each UIT bandpass, and comparing the results with UIT photometry, measured out to radii of ∼30″ to include all stellar flux. Statistical uncertainties in the mean *IUE*/UIT ratio thus derived are 0.06–0.08 mag, while internal uncertainty in UIT stellar photometry is 0.07 mag, from consistency checks on UIT data sets. The uncertainty in UIT photometry is therefore ∼0.10 mag relative to *IUE*, for stars brighter than our completeness limits of 14.0 for $m(162)$ and 14.5 for $m(249)$. [UIT magnitudes are defined by $m_\lambda = -2.5 \log (F_\lambda) - 21.1$, where F_λ is in ergs (cm^2 Å s)$^{-1}$.] We have also obtained ground-based images and photometry (Cheng et al. 1994), which may permit spectral type fitting (Hill et al. 1993) in later work.

3. DISCUSSION

3.1. *Magnitudes and Colors*

Figure 2*a* is the UIT color-magnitude diagram for the 1309 stars matched from 1729 on the NUV image and 1842 on the FUV image. No reddening corrections have been applied to observed data. Diamonds approximate stars with SMC com-

[1] Hughes STX Corporation, Code 681, Goddard Space Flight Center, Greenbelt, MD 20771.
[2] Space Telescope Science Institute, Homewood Campus, Baltimore, MD 21218.
[3] University of Virginia, Astronomy Department, P.O. Box 3818, Charlottesville, VA 22903.
[4] National Radio Astronomy Observatory, Edgemont Road, Charlottesville, VA 22903.
[5] Laboratory for Astronomy and Solar Physics, Code 680, Goddard Space Flight Center, Greenbelt, MD 20771.

PLATE L8

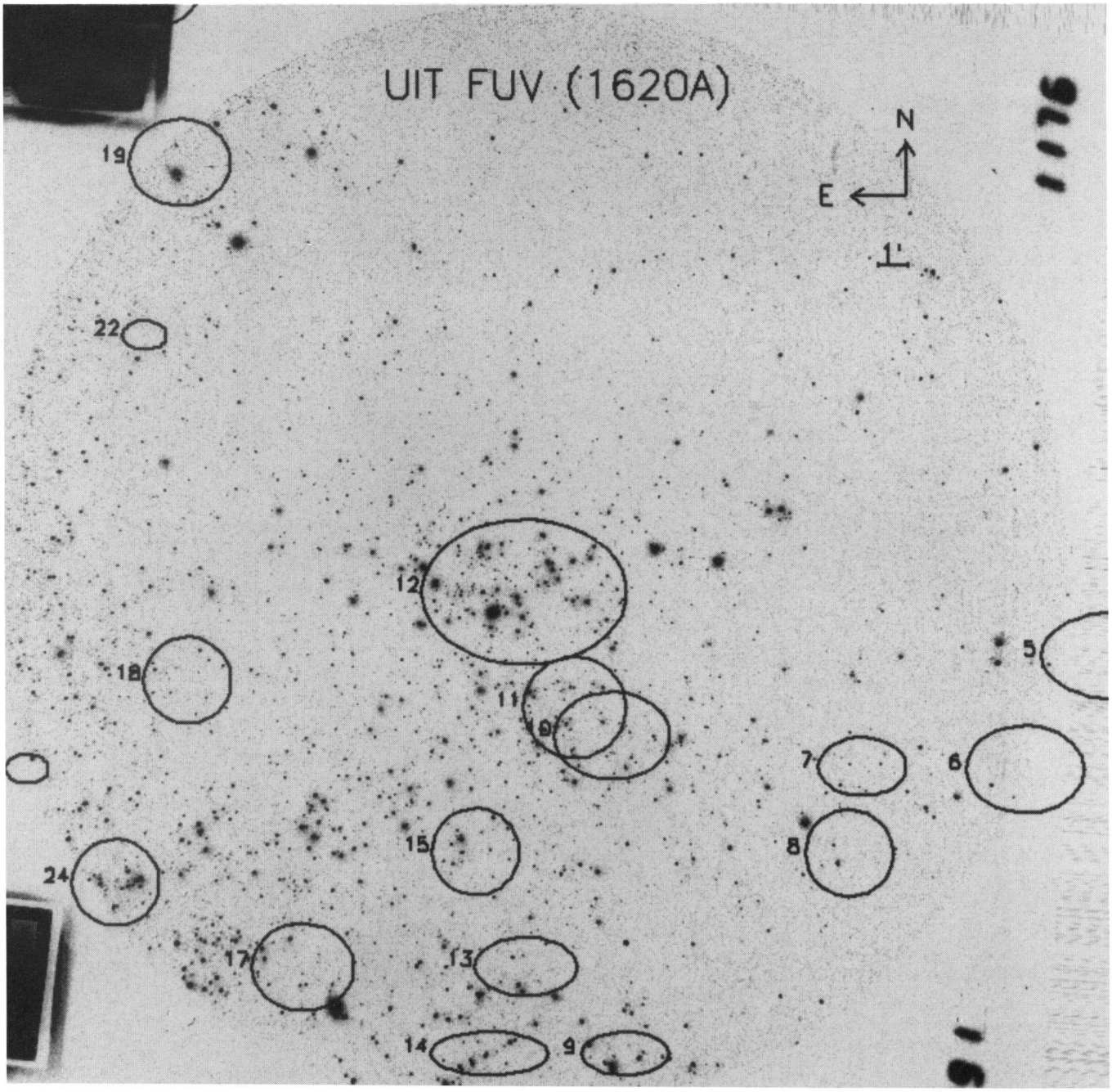

FIG. 1.—The UIT FUV (B5) 117 s image, with Hodge (1985) associations (as defined by positions and sizes in his Table I) outlined

position: magnitudes and colors are from model atmospheres of Kurucz (1993) with $\log (Z/Z_\odot) = -0.5$ ($\sim$solar/3.2), on stellar evolution models of Charbonnel et al. (1993) with $z = 0.004$ ($\sim$solar/5) and age 10 Myr. These grid points are selected as models with compositions nearest to the SMC value ($\sim$solar/4; Westerlund 1990). The supergiant "plume" of stars leaving the upper main sequence is visible parallel to the line connecting the 15 and 20 $M_\odot$ model points.

Circles connected by dashed lines are colors and magnitudes of main-sequence stars from the atlas of Galactic (unreddened) stellar spectra of Fanelli et al. (1992), with spectral classes from O3–6V to B5–8V. The $\sim$0.2 mag color offset between Galactic stars and SMC models shows the effect of line blanketing. Model and atlas stars are adjusted to distance modulus 18.9 and foreground Galactic extinction $E(B-V) = 0.02$ mag (Hutchings 1982). Reddening vectors for standard curves with $E(B-V) = 0.1$ are shown. The large $[m(162) - m(249)]$ color term of the SMC curve (Hutchings 1982)—$6.72 \times E(B-V)$ reddening versus $0.31 \times E(B-V)$ for the Galaxy—is evident. Other SMC extinction curves (Prevot et al. 1984 and references therein) are similar to the Hutchings curve, which we adopt, and are equivalent for our purposes. Typical optical-band $E(B-V)$ measurements of SMC field stars are represented by values for 20 stars measured by Hutchings, with $0.0 < E(B-V) < 0.13$, averaging 0.061 ± 0.037 (σ).

The observed stars clearly fit SMC-composition models better than Galactic spectra, since the SMC models lie at the blue edge of the observed stars, so that expected amounts of reddening will place the model stars at the observed positions in the diagram. We quantify this statement as follows. We compute the rms reddening in $[m(162) - m(249)]$ for observed stars that are bluer than the SMC models, as the distance along the SMC reddening vector from the 10 Myr isochrone: 0.159 mag. Similarly, the rms reddening computed for stars bluer than the Galactic-composition model locus is 0.268 mag. The rms uncertainty in observed $[m(162) - m(249)]$ color, computed from DAOPHOT PSF errors for the 1309 stars, is 0.106 mag. Therefore, SMC-composition models yield an observed scatter blueward of the model locus that is much closer to the expected value than do Galactic spectra. The increase in color scatter for fainter stars, expected for measurement errors, reinforces this conclusion. The difference between DAOPHOT results and observed scatter (0.106 vs. 0.159) may be explained by insufficiently blue SMC model colors, or underestimated photometric error for stars that are bluer than the model locus.

3.2. *Mass and Extinction Fitting*

In the $[m(162) - m(249), m(249)]$ plane of Figure 2, the SMC reddening vector is nearly perpendicular to the locus of main-sequence models. This geometry suggests that extinctions for observed stars may be derived by "dereddening" them to the model locus. We derive masses and extinctions for field stars by this technique, computing extinctions by moving the stars blueward to the isochrone, and masses from the resulting isochronal locations.

This procedure is clear for main-sequence stars. However, the supergiant branch is sensitive to isochrone age, and the resulting $E(B-V)$ values for bright stars vary considerably with that age. Therefore, the isochrone age is constrained by requiring a subset of stars that are clearly supergiants [$11.5 < m(249) < 13.0$; 116 stars] to have the same mean reddening as a subset of stars that are clearly on the main sequence and unaffected by completeness limits [$14.0 < m(249) < 14.5$; 243 stars]. Varying the latter limits has negligible effect on derived age and other results.

Two modifications to simple isochrones were developed and applied: (1) Because the field stars undoubtedly are not coeval, we have "aged" the lower main sequence, in effect assuming constant star formation. For each stellar mass model older than the isochrone age, we represent that mass by a model of half its main-sequence lifetime, representing each mass by stars

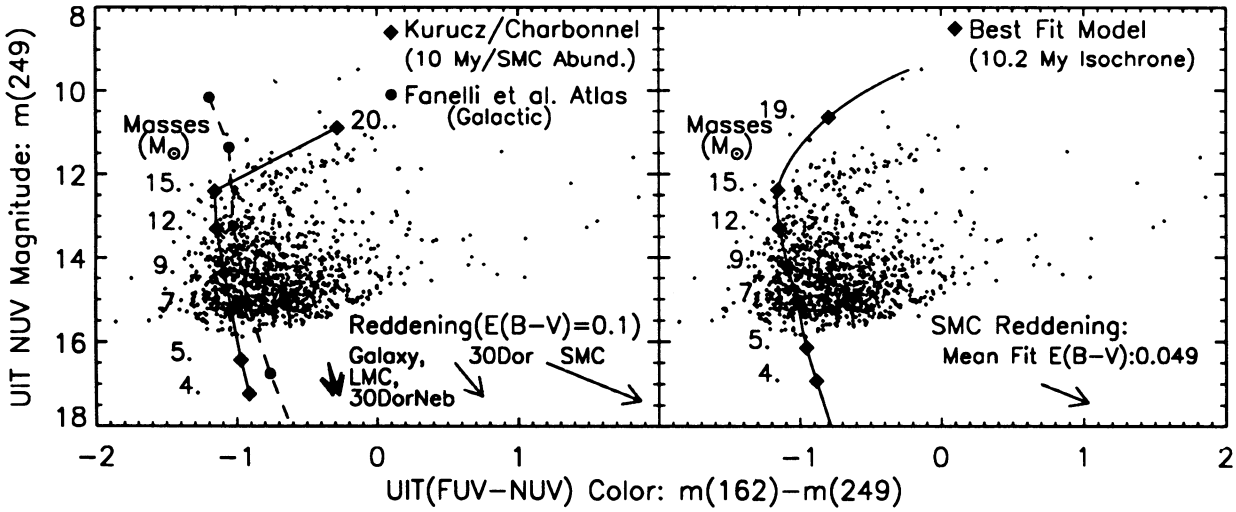

FIG. 2.—(*a*) The UIT color-magnitude diagram for 1309 stars in common between the FUV and NUV images. No reddening corrections are applied to observed points. Diamonds are models (masses labeled) with SMC composition ($\sim Z_\odot/4$). Filled circles connected by dashed lines are main-sequence stars from the atlas of Galactic stellar spectra of Fanelli et al. (1992). Model and atlas stars are adjusted to a distance modulus of 18.9 and $E(B-V) = 0.02$ Galactic foreground extinction. Reddening vectors for standard curves with $E(B-V) = 0.1$ are shown. (*b*) The UIT field color-magnitude diagram with the best-fit modified isochrone model superposed. Diamonds (masses labeled) are models with SMC composition, adjusted for distance, and Galactic foreground. The modified isochrone has a forced supergiant branch and "aged" main sequence as described in the text. The model age of 10.2 ± 1.0 Myr gives equal $\langle E(B-V) \rangle$ values for certain supergiants [$11.5 < m(249) < 13.0$)] and main-sequence stars [$14.0 < m(249) < 14.5$], and $\langle E(B-V) \rangle = 0.049$ mag, shown by the reddening vector plotted.

of average age for that mass. The result is models for $M < \sim 7$ $M_\odot$ that are ~ 0.1 mag redder in $[m(162) - m(249)]$ color and ~ 0.5 mag brighter in $m(249)$ than zero-age models. (2) Rapid supergiant branch evolution complicates interpolating models in that part of the diagram. Supergiant models with observed $m(162) - m(249) = -0.8$ are therefore generated by interpolating their mass and $m(249)$ values for each isochrone age from the initial model grid. The supergiant branch is then modeled by interpolating from the top of the main sequence through the $[m(162) - m(249) = -0.8, m(249)]$ point.

The resulting modified isochrone is represented by a spline fitted through the model points. The intersection of the isochrone and the reddening trajectory for each star is determined by an iterative numerical procedure. Models for ages of 3–13 Myr are computed, and the best fit is defined as described above, by requiring mean supergiant and main-sequence reddenings to be equal. The dereddened location on the modified isochrone determines the value of $E(B-V)$ and mass for each observed star.

Figure 2*b* shows results for a modified isochrone with our best fit for the field, assuming the SMC extinction function. The stellar models (diamonds, masses labeled) have SMC abundances and are reddened by the Galactic foreground value of $E(B-V) = 0.02$. All observed stars are dereddened by the iterative procedure onto the model locus within the width of the line connecting the models. The fit gives a modified isochrone age of 10.2 ± 1.0 Myr and a mean internal SMC extinction of $\langle E(B-V) \rangle = 0.049$, with the uncertainty primarily due to variations in isochrone shape caused by model grid granularity. For all fits we exclude ~ 40 stars with observed colors that are spuriously blue $[m(162) - m(249) < -1.4]$ or red $[m(162) - m(249) > 0.5]$. All others, even those with negative "reddenings," are retained.

The distribution of the amount of extinction in the field so derived shows very strong positional dependence. We group field stars into five bins by $E(B-V)$, with $0.0 \le E(B-V) < 0.024$, $0.024 \le E(B-V) < 0.048$, $0.048 \le E(B-V) < 0.072$, $0.072 \le E(B-V) < 0.096$, and $E(B-V) \ge 0.096$. The position centroids of the groups move monotonically from the NE to the SW by 6′ with increasing $E(B-V)$. This result is consistent with H I studies (e.g., Martin, Maurice, & Lequeux 1989), which find large H I depths and multiple features along the line of sight in the southwest SMC. Other field features also correlate with reddening. Stars within Hodge associations 10, 11, and 12 are generally lightly reddened, while a well-defined group of stars to the south is heavily reddened, perhaps lying farther along the line of sight within the SMC (cf. Westerlund 1990 and references therein).

The calculations also produce masses for the observed stars, which we use to compute an initial mass function for the observed field: a "present-day zero-age mass function" (PDZAMF). Interpreting the PDZAMF is complicated by at least two effects: (1) the field is not coeval, which biases the sample by stellar lifetime; and (2) extinction is significant for FUV observations and biases the sample with respect to stellar brightness. Stellar lifetime weighting is compensated conventionally, by dividing the number of stars in each mass bin by stellar lifetime. We compensate for extinction by determining magnitude limits for each image directly from magnitude distributions, and selecting only complete mass and extinction groups.

We therefore sort the observed stars by $E(B-V)$, and compute a PDZAMF only for stars with $0 < E(B-V) < 0.024$ (half the field mean reddening). Including SMC extinction of $E(B-V) = 0.024$, our mass completeness limit is 9 $M_\odot$, set by the $m(249)$ faint limit. We derive a PDZAMF slope of $\Gamma = -1.6$ (using logarithmic mass intervals, for which the Salpeter (1955) IMF slope is $\Gamma = -1.35$). This value is the result of a self-consistent solution for SMC field stars, given the Hutchings (1982) extinction function. No correction is made for binary or Wolf-Rayet stars, nor for incompleteness, other than restricting extinction as specified. Binary stars in any event would not affect our data as much as optical studies because of the relatively small likelihood of binary stars with two UV-bright components.

We have explored the range of reasonable Galactic foreground extinction. $E(B-V) = 0.02$ is at the lower end of the accepted range (Westerlund 1990). Since the FUV and NUV bandpasses have nearly equal Galactic extinctions for hot stars [$8.06 \times E(B-V)$ and $7.75 \times E(B-V)$ respectively], variations in foreground extinction should have little effect on colors and model results. Model calculations confirm this; doubling the Galactic foreground value to 0.04 has negligible effect on the derived age or $\langle E(B-V) \rangle$ for the field.

3.3. *Variations in the Extinction Function and the PDZAMF*

The Galactic interstellar extinction function varies among lines of sight (Witt, Bohlin, & Stecher 1984) and is widely believed to depend on dust composition and thus on evolutionary conditions (e.g., Mathis, Rumpl, & Nordsieck 1977). For example, Witt, Bohlin, & Stecher (1984) determine 1250 and 2160 Å extinctions of 29 Galactic stars from *IUE* spectra and find that stars associated with dense interstellar clouds have significantly weaker extinction for $\lambda < 2500$ Å than stars associated with diffuse clouds; large dispersions in $E(\lambda - V)/E(B-V)$ ($\sigma = 1.45$ for 1250 Å and 0.59 for 2160 Å) are derived for the complete sample. Also, the mean SMC extinction curve, derived from a few stars, may represent only part of the SMC ISM. Studies of extinction in the SMC ISM should consider the likely case that deviations from accepted parameters occur as a result of local variations in composition or evolutionary state.

In this section, we study the dependence of our model results on extinction function parameters. A grid of best-fit isochrone models is derived, with mass and $E(B-V)$ distributions for each parameterization. To constrain the models, we require (1) $E(B-V)$ values derived from UV measurements that are consistent with optical-band measurements; (2) reasonable mass functions; and (3) FUV and NUV extinction curve parameters which are consistent with values measured in the SMC and elsewhere.

Figure 3 shows the dependence of PDZAMF slope (solid-line contours labeled with $-\Gamma$ values) on $A[m(162)]/E(B-V)$ and $A[m(249)]/E(B-V)$, which we call R_{FUV} and R_{NUV}, respectively. Figure 3 also shows how constraints on optical extinction, PDZAMF slope, and R_{FUV} and R_{NUV} intersect to determine a range of acceptable solutions. Models are computed for integer values of R_{FUV} and R_{NUV} for all points with $R_{NUV} \le R_{FUV}$. (Cases for $R_{NUV} > R_{FUV}$ are omitted since for these values positive extinction moves the stars redward, away from the stellar model colors.) Solid contours outline model-derived PDZAMF slopes, while the shaded region covers model-derived $\langle E(B-V) \rangle$ values within the observed SMC range, which we take as $0.03 < E(B-V) < 0.08$ (Westerlund 1990). R_{NUV} and R_{FUV} values observed in the SMC (diamond),

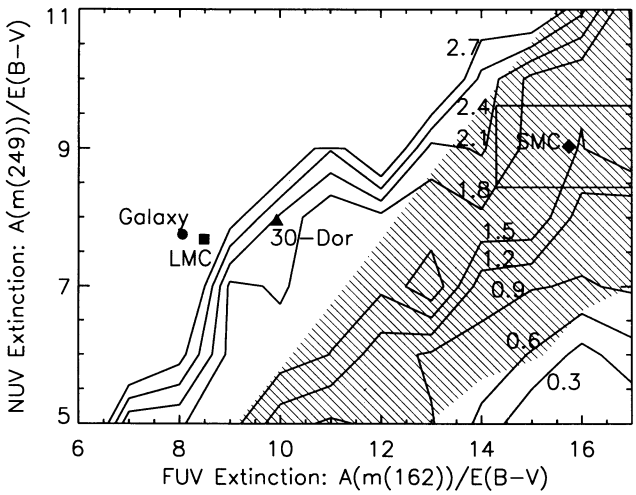

FIG. 3.—Contours of model-derived present-day, zero-age mass function (PDZAMF) slope (solid contours, labeled with $-\Gamma$) as a function of $A[m(162)]/E(B-V)$ ($\equiv R_{FUV}$) and $A[m(249)]/E(B-V)$ ($\equiv R_{NUV}$). The shaded region covers parameters which produce mean $E(B-V)$ values within accepted optically derived limits for SMC field stars [$0.03 < E(B-V) < 0.08$; Westerlund 1990]. Accepted R_{FUV} and R_{NUV} values for the SMC (*diamond*), Galaxy (*circle*), 30 Dor region (*triangle*), and general LMC (*square*) are also shown. To demonstrate expected extinction parameter variations the SMC point is surrounded with a box defining the 1 σ variations for Galactic stars at wavelengths near 1620 and 2490 Å from Witt, Bohlin, & Stecher (1984). Note (*a*) SMC extinction parameters are the only observed ones which produce $\langle E(B-V)\rangle$ near the acceptable range, and (*b*) extinction parameters over a large range near SMC values produce PDZAMF slopes in the accepted range of $\Gamma = -1.7 \pm 0.5$ (Scalo 1986).

Galaxy (circle), 30 Dor region (triangle), and general LMC (square) are also shown. Expected extinction parameter variations at 1620 and 2490 Å, respectively, are approximated by surrounding the SMC point with a box the size of the 1 σ dispersions observed for the Galactic extinction law at 1250 and 2160 Å by Witt, Bohlin, & Stecher (1984).

Figure 3 establishes immediate conclusions. First, only extinction functions with parameters near SMC values produce models with mean $E(B-V)$ in the observed range. Model-derived $\langle E(B-V)\rangle$ is inversely related to the reddening between 1620 and 2490 Å, $C' = R_{FUV} - R_{NUV}$, since observed stars must be dereddened by $m(162) - m(249) \sim 0.5$ on average. The upper edge of the shaded region, defined by $E(B-V) = 0.08$, lies nearly along the $C' = 4$ locus, and the lower edge is at $E(B-V) = 0.03$ and $C' \sim 8$–9. Therefore, only large C' values produce derived mean $E(B-V)$ as small as are observed in the SMC. Our results thus are strong evidence for an SMC extinction function which rises steeply between the NUV and FUV bandpasses, like that of Hutchings (1982), which has $C' = 6.72$. This function is unlike others found to date ($C' = 1.99$ for 30 Dor, and $C' < 1.0$ for all others).

Second, reasonable PDZAMF slopes ($\Gamma = -1.7 \pm 0.5$; Scalo 1986) cover a large range of UV extinction parameters. Models with slopes in this range are distributed like those with acceptable $\langle E(B-V)\rangle$, but trail to smaller C' for small R_{NUV}. Consequently, the box which defines reasonable deviations from the SMC extinction point is completely contained within reasonable PDZAMF values, implying that PDZAMF slopes in this range hold more generally than particular extinction parameters. Our SMC models therefore permit significant variation in extinction parameters while maintaining a relatively uniform PDZAMF slope, as seen under a wide variety of evolutionary circumstances and abundances (Scalo 1986; Larson 1991; Parker & Garmany 1993; Malamuth & Heap 1994; Hill et al. 1994).

Our results support Scalo (1986), Larson (1991), and others, who conclude that the observed IMF is relatively uniform for field stars more massive than a few $M_\odot$ and is well represented by a power law with slope near -1.7. (In OB associations such as 30 Dor where conditions and perhaps dominant physical processes are different, this may not be true; cf. Malamuth & Heap 1994 and Hill et al. 1994). Characteristics of dust certainly vary throughout the observed universe, probably with the overall evolutionary state of the local ISM. For example, the lack of a 2200 Å absorption feature in the SMC may be due to the relative scarcity of evolved stars which have dredged up and expelled carbon-rich core material. The variation of extinction laws within the Galaxy, the extreme case of the accepted SMC curve, and the intermediate values in the LMC and 30 Dor region clearly point to UV extinction which "flattens" (and gains a 2200 Å feature) as the ISM gains heavy elements. However, our results (Fig. 3) show that this variation does not appreciably affect the field mass function slope derived using UV data. The PDZAMF slope is therefore a relatively fixed quantity throughout the local universe, depending as it does on the universal physics of single-star formation; while characteristics of local dust vary, depending critically on local ISM composition and evolutionary state.

We thank Robert S. Hill for several useful discussions. Funding for the UIT project has been through the Spacelab Office at NASA Headquarters under Project Number 440-51.

REFERENCES

Bohlin, R. C., Harris, A. W., Holm, A. V., & Gry, C. 1990, ApJS, 73, 413
Charbonnel, C., Meynet, G., Maeder, A., Schaller, G., & Schaerer, D. 1993, A&AS, 101, 415
Cheng, K.-P., et al. 1994, in preparation
Fanelli, M. N., O'Connell, R. W., Burstein, D., & Wu, C. C. 1992, ApJS, 82, 197
Hill, J. K., Bohlin, R. C., Cheng, K-P., Fanelli, M. N., Hintzen, P., O'Connell, R. W., Roberts, M. S., Smith, A. M., Smith, E. P., & Stecher, T. P. 1993, ApJ, 413, 610
Hill, J. K., Isensee, J. E., Cornett, R. H., Bohlin, R. C., O'Connell, R. W., Roberts, M. S., Smith, A. M., & Stecher, T. P. 1994, ApJ, 425, 122
Hodge, P. W. 1985, PASP, 97, 530
Hutchings, J. B. 1982, ApJ, 255, 70
Kurucz, R. L. 1992, in The Stellar Populations of Galaxies, ed. B. Barbuy & A. Renzini (Dordrecht: Kluwer), 225
Larson, R. B. 1991, in Fragmentation of Molecular Clouds and Star Formation, ed. E. Falgarone, F. Boulanger, & G. Duvert (Dordrecht: Kluwer), 261
Lasker, B. M., Sturch, C. R., McLean, B. J., Russell, J. L., Jenkner, H., & Shara, M. M. 1989, preprint
Malamuth, E. M., & Heap, S. R. 1994, AJ, 107, 1054
Martin, N., Maurice, E., & Lequeux, J. 1989, A&A, 215, 219
Mathis, J. S., Rumpl, W., & Nordsieck, K. H. 1977, ApJ, 217, 425
Parker, J. W., & Garmany, C. D. 1993, AJ, 106, 1471
Prevot, M. L., Lequeux, E., Maurice, L., Prevot, L., & Rocca-Volmerange, B. 1984, A&A, 132, 389
Salpeter, E. E. 1955, ApJ, 121, 161
Scalo, J. M. 1986, Fund. Cosmic Phys., 11, 1
Stecher, T. P., et al. 1992, ApJ, 395, L1
Stetson, P. B. 1987, PASP, 99, 101
Westerlund, B. E. 1990, Astron. Ap. Rev., 2, 29
Witt, A. N., Bohlin, R. C., & Stecher, T. P. 1984, ApJ, 279, 698